UNCLASSIFIED

AD NUMBER
AD338967
CLASSIFICATION CHANGES
TO: **UNCLASSIFIED**
FROM: **CONFIDENTIAL**
LIMITATION CHANGES
TO: **Approved for public release; distribution is unlimited.**
FROM: **Distribution authorized to U.S. Gov't. agencies and their contractors; Administrative/Operational Use; 26 JUN 1963. Other requests shall be referred to Defense Atomic Support Agency, Washington, DC.**
AUTHORITY
DNA ltr 21 Dec 1984; DNA ltr 21 Dec 1984

THIS PAGE IS UNCLASSIFIED

AD- 338967

SECURITY REMARKING REQUIREMENTS

DOD 5200.1-R, DEC 78

REVIEW ON 26 JUN 83

UNCLASSIFIED

AD 338967

CLASSIFICATION CHANGED
TO: UNCLASSIFIED
FROM CONFIDENTIAL
AUTHORITY: DNA ltr
21 Dec 84

UNCLASSIFIED

CONFIDENTIAL

AD 338967

DEFENSE DOCUMENTATION CENTER

FOR

SCIENTIFIC AND TECHNICAL INFORMATION

CAMERON STATION, ALEXANDRIA, VIRGINIA

CONFIDENTIAL

Best

Available

Copy

CONFIDENTIAL

Operation

SUN BEAM

SHOT SMALL BOY

(U)

POR-2241
(WT-2241)

This document consists of 58 pages

No. 1__ of 255 copies, Series A

PROJECT OFFICERS REPORT—PROJECT 7.5

RESPONSE OF ELECTRICAL POWER SYSTEMS TO ELECTROMAGNETIC EFFECTS OF NUCLEAR DETONATIONS (U)

D. B. Dinger, Project Officer

R. J. Bostak

U. S. Army Engineer Research and Development Laboratories
Fort Belvoir, Virginia

AD NO. 338967

DDC FILE COPY

Issuance Date: June 26, 1963

CONFIDENTIAL

Inquiries relative to this report may be made to

Chief, Defense Atomic Support Agency
Washington 25, D. C.

When no longer required, this document may be destroyed in accordance with applicable security regulations.

DO NOT RETURN THIS DOCUMENT

B 1 1 400 N

CONFIDENTIAL

POR-2241
(WT-2241)

OPERATION SUN BEAM

SHOT SMALL BOY

PROJECT OFFICERS REPORT—PROJECT 7.5

RESPONSE OF ELECTRICAL POWER SYSTEMS TO ELECTROMAGNETIC EFFECTS OF NUCLEAR DETONATIONS (U)

D. B. Dinger, Project Officer

R. J. Bostak

U.S. Army Engineer Research and Development Laboratories
Fort Belvoir, Virginia

DEPARTMENT OF DEFENSE
WASHINGTON 25, D. C.

CONFIDENTIAL

ABSTRACT

The response of a typical field army electrical power system to the electromagnetic pulse was measured at sufficient distance from ground zero to prevent damage from blast and thermal effects. Twenty channels of a recording oscillograph were used to monitor selected variables from ~~minus~~ − 15 seconds to ~~plus~~ + 15 seconds and to provide fiducial indications.

From analysis of the data, it was determined that the electrical power system was shut down by a combination of effects such as prompt radiation and effects of the electromagnetic pulse. A failure mechanism theory was postulated. Laboratory investigation verified the basic theory. Further laboratory investigation, analog computer analysis, and transient circuit analysis were conducted to determine the characteristics of the current pulse introduced by the power cable necessary to result in the failure mechanism. If induced currents in the distribution cable were the only cause of power system shutdown, a current pulse of approximately 3570 amperes maximum would be required. ~~The results~~ ~~of~~ this experiment will be applied to a related Nuclear Weapons Effects Research program at U.S. Army Engineer Research and Development Laboratories (USAERDL).

CONTENTS

CHAPTER 1

INTRODUCTION

1.1 OBJECTIVE

The objective of this project was to determine the degree of protection necessary to result in field army electrical power systems that will remain within performance tolerances when subjected to the electromagnetic effects of nuclear detonations when located at sufficient distances from the detonation point to assure little or no physical damage to the electrical power system due to blast and thermal effects.

1.2 BACKGROUND

1.2.1. Army Requirements. The Electrical Power Branch of the Engineer Research and Development Laboratories (ERDL) is engaged in research and development of electrical power generation equipment for the US Army. Contemporary power generation equipment includes gasoline-engine-driven generator sets rated from 0.15 to 10 kw, diesel-engine-driven generator sets rated from 15 to 150 kw, and special purpose gasoline-engine-driven, diesel-engine-driven, and gas turbine generator sets of various ratings for use as ground support equipment in mobile missile systems. A typical field army electrical power system consists of a power generation device, distribution cables, and electrical loads.

Field army electrical power systems are extremely vulnerable to the electromagnetic pulse from a nuclear detonation because the distribution cables act as excellent antennas for the very high-amplitude, low-frequency fields generated by the detonation. The military situation of primary interest is that in which a nuclear detonation has occurred at sufficient distance from a missile support complex, of which the field army electrical power system is a component, to assure little or no physical damage to the complex. Considering the peak magnitudes of the electric and magnetic fields at distances from the detonation point commensurate with the above military situation, it is highly feasible that the electrical power system will become inoperable at the time when most needed for retaliatory purposes, if no more than ordinary design methods are used in the interconnecting power distribution cables. It is considered necessary to investigate the response of a field army electrical power system to the excitation of the electromagnetic pulse from a nuclear detonation in order to determine the degree of protection necessary to result in satisfactory system operation in this electromagnetic environment.

1.2.2 Results from Previous Projects. The electromagnetic effects are probably the least known of all the major effects of near-surface nuclear weapon detonations. This situation has come about because the electromagnetic phenomenon was considered to be a nuisance effect rather than a weapons effect during the early series of full scale nuclear detonations.

Consequently, measures were taken to replace the damaged cables, galvanometers, and other equipment, and to protect insufficiently shielded instruments from unwanted signals. No major effort was formulated to investigate the electromagnetic phenomenon and evaluate its military significance.

Projects have subsequently been conducted for the purpose of measuring the magnetic field component and the electric field component of the electromagnetic field from nuclear detonations. Additional projects were conducted during Shot Small Boy and other contemporary full-scale operations for the purpose of verifying previous data and gaining further insight into the basic nature of the electromagnetic pulse. A fundamental goal of the basic field studies was to formulate empirical and analytical representations as a function of distance, time, and yield.

1.3 THEORY

The above empirical and analytical relationships can be used in a theoretical analysis of the effects of the electromagnetic pulse on equipment. However, the need existed for the conduct of an experiment to determine the operational response of the system under study to the excitation of a known electromagnetic pulse created by a nuclear detonation. This opportunity was afforded during Shot Small Boy, as the basic electromagnetic field was being measured by other projects. It was believed that correlation of the operational data derived from Project 7.5 with corresponding basic electromagnetic field data determined by other projects would result in quantitative information relevant to theoretical analysis of the effects of the electromagnetic pulse on electrical power systems, which would in turn result in determination of protective techniques.

The basic approach followed was to locate a typical field army electrical power system at sufficient distance from ground zero (GZ) to prevent physical damage due to blast and thermal effects and to monitor the performance of selected currents and voltages during the predetonation steady-state period, during the postdetonation transient period, and during the postdetonation steady-state period. The engine-generator set schematic diagram was examined to determine the currents and voltages to be monitored. Monitored variables were chosen to result in a definitive record of system response to the electromagnetic pulse and to pinpoint the failure mechanism. Variables chosen reflected generator set performance with regard to output, excitation, and control. Reference values for the monitored variables were established during the predetonation steady-state period. The electrical power system was considered, for the purpose of analysis, to be a physical entity to which the electromagnetic pulse I(t) was applied as shown in Figure 1.1. The response of each monitored variable $R_1(t)$, $R_2(t)$ ------$R_{17}(t)$ was considered to be a perturbation about the corresponding reference value.

A loop antenna was designed to provide a zero-time reference for the arrival of the electromagnetic pulse. Data from previous experiments (Reference 1) indicated that the magnetic field intensity $\vec{H}$ and the derivative of the magnetic field intensity with respect to time $\frac{d\vec{H}}{dt}$ would be maximum in the $\vec{A}_\phi$ direction, where ϕ is the azimuthal angle of the spherical coordinate system shown in Figure 1.2 in which a point in space is specified by r (the radial distance from the origin), θ (the polar angle), and ϕ (the azimuthal angle). For GZ located at the origin, the point P_2 corresponds to the location of Project 7.5. The polar angle θ is approximately equal to 90 degrees, and the spherical coordinate system of Figure 1.2 can be represented by the polar coordinate system of Figure 1.3.

The loop antenna was oriented so that the vector normal to its area coincided with the unitary base vector $\vec{A}_\phi$ of Figure 1.3. The output of the loop antenna was predicted by utilizing Faraday's Law as follows:

$$e = -N\frac{d\Psi}{dt} = -N\mu A\frac{dH_\phi}{dt} \qquad (1.1)$$

Where: e = induced voltage, volts

N = number of turns

Ψ = total magnetic flux, webers

μ = permeability of free space, $4\pi(10)^{-7}$ henry/m

A = loop aperture area, m^2

$\frac{dH_\phi}{dt} = \frac{\text{ampere-turns}}{\text{m sec.}}$

An empirical formula derived from previous full-scale testing was used to calculate $\frac{dH_\phi}{dt}$ (Reference 2).

The electrical power system was oriented at 45 degrees with respect to the radius vector from GZ, with the electrical load closer to GZ than the power generation device.

This orientation was chosen to result in an intermediate contribution of induced voltage and currents to the generator set from the load cable and was believed to be most advantageous for the study of the response of the entire system.

Due to stringent deadlines present throughout the project preparation period, the major efforts of project personnel were necessarily directed toward the design, development, test-in, and field implementation of an effective experimental system. However, a corresponding analytical program was considered essential for a comprehensive analysis of data resulting from this experiment and a quantitative investigation of the field army electrical power system electromagnetic pulse problem. This analytical program was initiated as a supplementary portion of this experiment and is being continued as part of a Nuclear Weapons Effects Research Program at U.S. Army Engineer Research and Development Laboratories (USAERDL).

The basic goal of this analytical program is to determine the response of a power cable, with physical and electrical characteristics typical of a field army application, to the incident electromagnetic pulse. The problem is essentially that of the interaction of a transverse magnetic wave with a circular cylindrical conductor embedded in dielectric media. The case of waves that are predominantly transverse magnetic corresponds to the important problem of axial current in the cylindrical conductor (Reference 3). Characteristics of the incident wave are dependent upon experimental data obtained during the Small Boy shot and previous nuclear weapons effects testing.

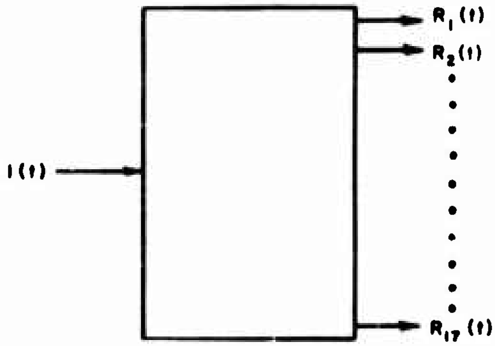

Figure 1.1 Block diagram representation of project.

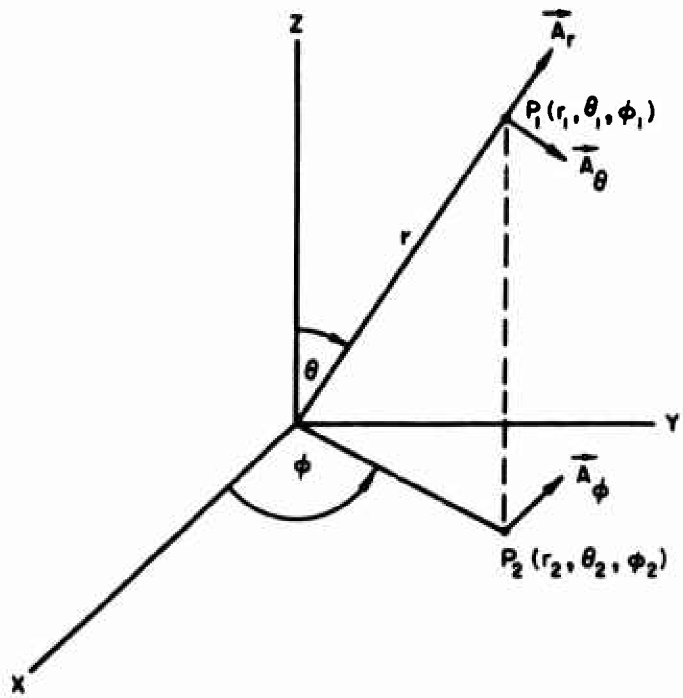

Figure 1.2 Spherical coordinate system.

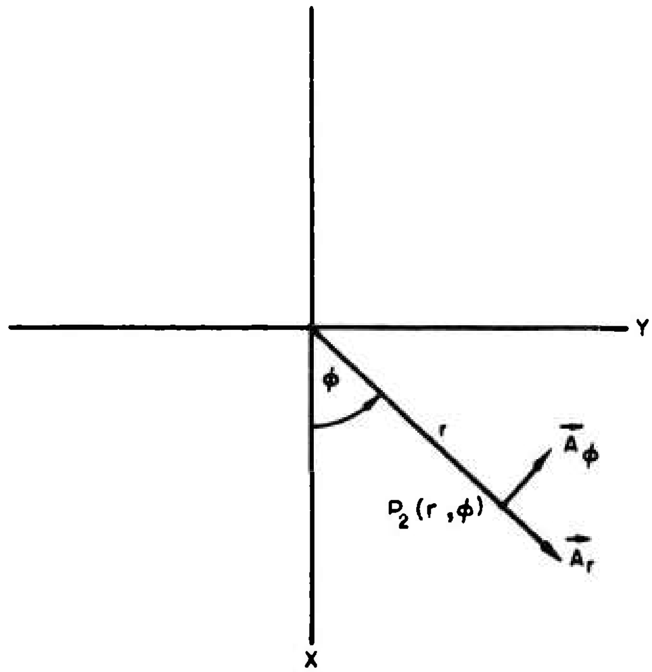

Figure 1.3 Polar coordinate system.

CHAPTER 2

PROCEDURE

2.1 OPERATIONS

The project layout is shown in Figures 2.1 through 2.3. The field army electrical power system consisted of a 45-kilowatt, 400 cps, engine-generator set, sufficient resistive and reactive load to permit system operation at rated load and rated power factor, and two 120-foot distribution cables. Upon evacuation of the area, the generator set was operating at rated load and rated power factor from the auxiliary fuel source, and the instrumentation system was deenergized. A sequence of timing signals delivered by hardwire lines was used to activate and control the performance of selected control circuitry and the generator set output throughout the predetonation period and postdetonation period under study. Two devices were used to provide fiducial markers on the oscillogram. The output of a loop antenna was used to signify arrival of the electromagnetic pulse. A pressure-sensitive device was used in conjunction with electrical circuitry to provide zero time reference for shock wave arrival. A limit switch was used to deactivate the instrumentation system and the electrical power system at the conclusion of the monitoring period. Recovery of data consisted of removing the oscillogram from the oscillograph.

2.2 INSTRUMENTATION

2.2.1 Equipment. Sufficient resistive and reactive load to permit system operation at rated load and rated power factor, two 120-foot, 28 conductor distribution cables, and a 45 kilowatt, 400 cps engine-generator set, constituted the field army electrical power system. The distribution cables, which were unshielded and rubber covered, are typical of those used in field army electrical power installations. The engine generator set under study (which had a static excitation system and an electric load sensing governor) is representative of those currently issued for use by the field army in missile complexes and other applications where precise quality electrical power is required. Signals proportional to the monitored variables were passed through a plug board located on the generator set and transmitted to the recording circuitry by means of a transmission line. The generator set and associated instrumentation are shown in Figure 2.4. The generator set schematic diagram is shown in Figure 2.5. In order to prevent having the power system deenergized by a relatively unimportant malfunction during the period of unattended operation, the emergency operation switch (S7 in Figure 2.5) was reversed. This bypassed the relay contacts corresponding to the fuel pressure (FP), oil pressure (OP), and water temperature (WT) protective devices. The overspeed device relay contacts (OS) were also bypassed.

Development of an instrumentation system that would satisfactorily monitor the operation of the field army electrical power system throughout the predetonation steady-state period, the postdetonation transient period, and the postdetonation steady-state period presented many challenging problems. Figure 2.6 contains a block diagram representation of the instrumentation system. The initial procedure in instrumentation system development was determination of the required characteristics for the recording device, about which the system was designed.

The frequency components of the expected signal, the characteristics of the electrical power system, and the ambient environment determined the following required characteristics for the recording devices: (1) sufficient recording time to allow monitoring of predetonation steady-state, postdetonation transient, and postdetonation steady-state engine generator set performance assuming the instrument had been turned on previously by a timing signal, (2) completely self-powered since power lines could serve as source antennas to introduce unwanted signals into the instrument, (3) capable of withstanding and recording through the accelerating forces caused by the passing shock wave, (4) capable of simultaneously recording the signals from a minimum of nineteen signal sources, and (5) sufficient electromagnetic shielding so that the large electric field could not become impressed directly on the recording circuitry. The Consolidated Electrodynamics Corporation's oscillograph (Model 5-119P450) that was chosen for this application operates at a maximum film speed of 160 in/sec and has a fifty-channel recording capacity. This type of recorder has been used in previous shots. The special shock mount will withstand accelerations up to 3g. Total recording time was about 30 seconds on 12-inch film. The choice of galvanometers involved a compromise between frequency range and sensitivity. The galvanometers (Consolidated Electrodynamics Corporation, Type 7-326) have a flat frequency range from 0-3000 cps $\pm$ 5 percent and a system voltage sensitivity of 3.44 volts/in. These characteristics were consistent with the signal levels and frequency components to be measured in most cases. In some circuits, it was necessary to use galvanometers with greater sensitivity due to low signal levels.

A comprehensive analysis of the engine-generator set was conducted to determine the optimum variables to be monitored. The criterion employed throughout the above analysis was that study of the monitored variables must result in a definitive representation of engine-generator set performance. Signals proportional to the monitored variables pass through various attenuation and damping networks to the galvanometers. Resistance values required to provide proper galvanometer damping were calculated by analyzing the output impedance of the galvanometer circuits. Balancing techniques were employed in the galvanometer circuits to discriminate against unwanted signals.

A timing oscillator was developed to provide an accurate time reference on the oscillogram for use in analysis. The integral oscillograph timing motor was inadequate due to inaccuracies at high film speed caused by fluctuation of the supply voltage.

The function of the remainder of the instrumentation system was to control the recording device discussed above. The oscillograph power supply consisted of an integral direct current power supply, an inverter, and an autotransformer (for voltage gain). Four 12-volt, 45-ampere-hour batteries comprised the direct current supply. In order to provide maximum hold time throughout the period of instrumentation system activation, the generator set battery charging generator maintained the power supply batteries in a state of maximum charge until this circuit was opened as part of the operational sequence.

A loop antenna was developed to provide a galvanometer deflection that was a zero time reference for the arrival of the electromagnetic pulse. Twenty turns of conductor were used in the antenna, which was of four-foot diameter.

Four timing signals provided by hardwire lines were utilized to control instrumentation system relays which performed switching functions. The schematic diagram for the control relays is shown in Figure 2.7. At H-30 minutes, the oscillograph was activated and placed in the power-on mode of operation through the action of a timing signal. This warmup time was required to stabilize the galvanometer block temperatures on the oscillograph. The battery-charging generator was disconnected by a timing signal at H-30 seconds. At H-15 seconds, the action of a timing signal placed the oscillograph in the run mode of operation. A timing signal at H-5 seconds was used to activate a detonation circuit which opened the external timing lines and thus placed the instrumentation system in completely autonomous operation. Opening the external lines was necessary to prevent system inputs from the timing lines, which are excellent antennas for the electromagnetic pulse. The complete operational sequence is shown in Table 2.1.

The 20-foot-long transmission line from the generator set to the instrumentation container consisted of 27 shielded conductor pairs with two additional flexible concentric shielded conductors. The outer conductors served as a magnetic shield and provided a better-than-98-percent shielding factor against static magnetic fields. The shielding factor against electromagnetic fields was considerably better and increased with frequency.

The oscillograph, with its associated power supply and control circuitry, was mounted in an aluminum inclosure, which formed a cube approximately 3 feet on each side. The inclosure was hinged at one end and could be opened to provide easy access for servicing. A double mumetal shield of 31-mil thickness completely surrounded this package and was separated from it by a layer of felt on all sides and bottom. An exterior shielding box of 1/8-inch Armco iron with interior dimensions of 42 by 45 by 50 inches surrounded the mumetal shield, and a layer of compressed felt separated the two. The instrumentation package is shown in Figure 2.8, with the outer and inner doors opened.

The calculated electromagnetic shielding factor of the three-box assembly was 10^{10} at 1,000 cps. While this may appear to have been over-designed, it must be remembered that, due to the high wave impedance of the near field, the electric field was predicted to have a value of approximately 10^4 v/m; a shielding factor of 10^{10} would reduce this to 1.0μ v/m, which was considered acceptable.

The transmission line was connected by quick-break connectors to the aluminum box. The aluminum inclosure could be pulled out through the top opening of the shielding boxes to gain access to the oscillograph for servicing.

2.2.2 Calibration. Calibration was performed before installation of the station in order to obtain magnitudes of the reference values of the monitored variables. Since the characteristics of the galvanometers were known, the magnitude of the variation of each variable during the transient period could be calculated as follows:

$$e(t) = (s)(d)(x) \tag{2.1}$$

Where:

$e(t)$ = magnitude of variable at any time t, units

s = galvanometer voltage sensitivity, volts/inch

d = amount of deflection, inches

x = calibration constant, units/volt

2.2.3 Method of Installation and Recovery. The recorder boxes had to be protected from the effects of overpressure, and although the oscillograph was capable of operating under the anticipated acceleration, it was desirable to reduce the shock to a minimum by a suitable shock mount. Furthermore, the electronic circuits had to be protected from neutron and gamma radiation, since the former would damage components as well as induce gamma radiation by capture processes in some of the materials used (making recovery more difficult), and the latter would be the equivalent of a flow of charge that would create unwanted signals within the instrumentation.

Subsurface installations were therefore planned, and calculations were made to determine the depth necessary to protect the instrument from the above mentioned environments. The pit measured approximately 7 feet to the surface. To accommodate the instrumentation box, the pit was 5 feet square. For best results, the entire space above the instrumentation should have been filled with soil; this, however, would have introduced a serious recovery problem. Instead, sandbags grouped together were used as the cover, and care was taken not to leave large voids through which neutron leakage could occur.

A cross-sectional drawing of the station is shown in Figure 2.9, with dimensions as shown. The instrument box is shown on the bottom, supported by a polyurethane-plywood sandwich. A wooden platform, which rested on the shelf shown in

Figure 2.9, was constructed to accommodate the sandbags and facilitate placement and removal. The transmission line was placed through openings in the layers of sandbags and extended up to the distribution panel on the generator set.

TABLE 2.1 OPERATIONAL SEQUENCE

TIME	OPERATION
Minus 30 minutes	Timing signal relay closed. Oscillograph placed in power-on status.
Minus 30 seconds	Timing signal relay opened. Battery charging generator circuit opened.
Minus 15 seconds	Timing signal relay closed. Oscillograph placed in run status (began recording).
Minus 5 seconds	Timing signal relay closed. Timing signal external lines opened.
Plus 15 seconds	Limit switch on film drum opened. Oscillograph and generator set de-activated.

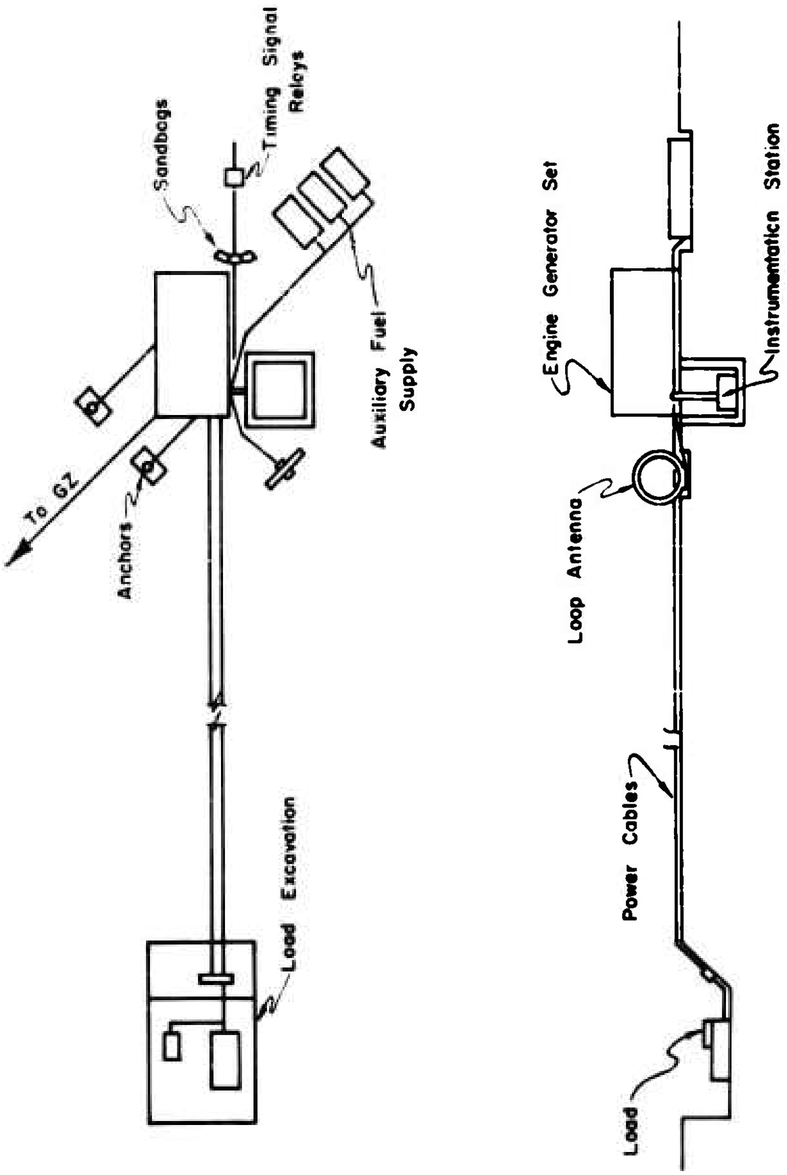

Figure 2.1 Project layout.

Figure 2.2 Resistive and reactive load bank. (USAERDL photo)

Figure 2.3 Instrumentation and power generation facility. (USAERDL photo)

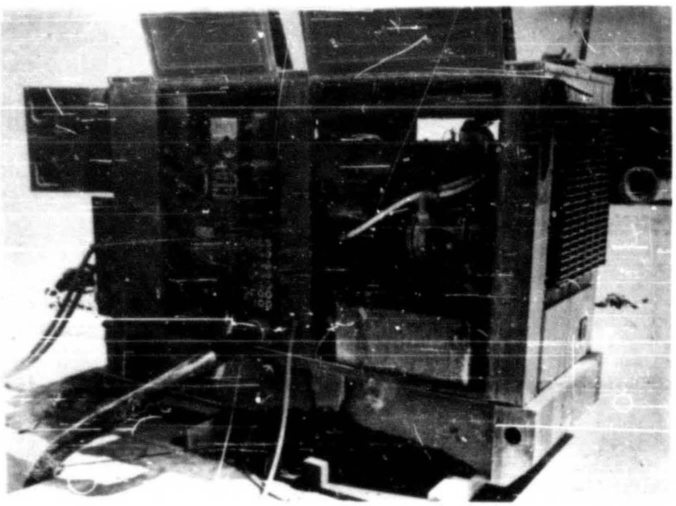

Figure 2.4 Power generation unit and associated instrumentation. (USAERDL photo)

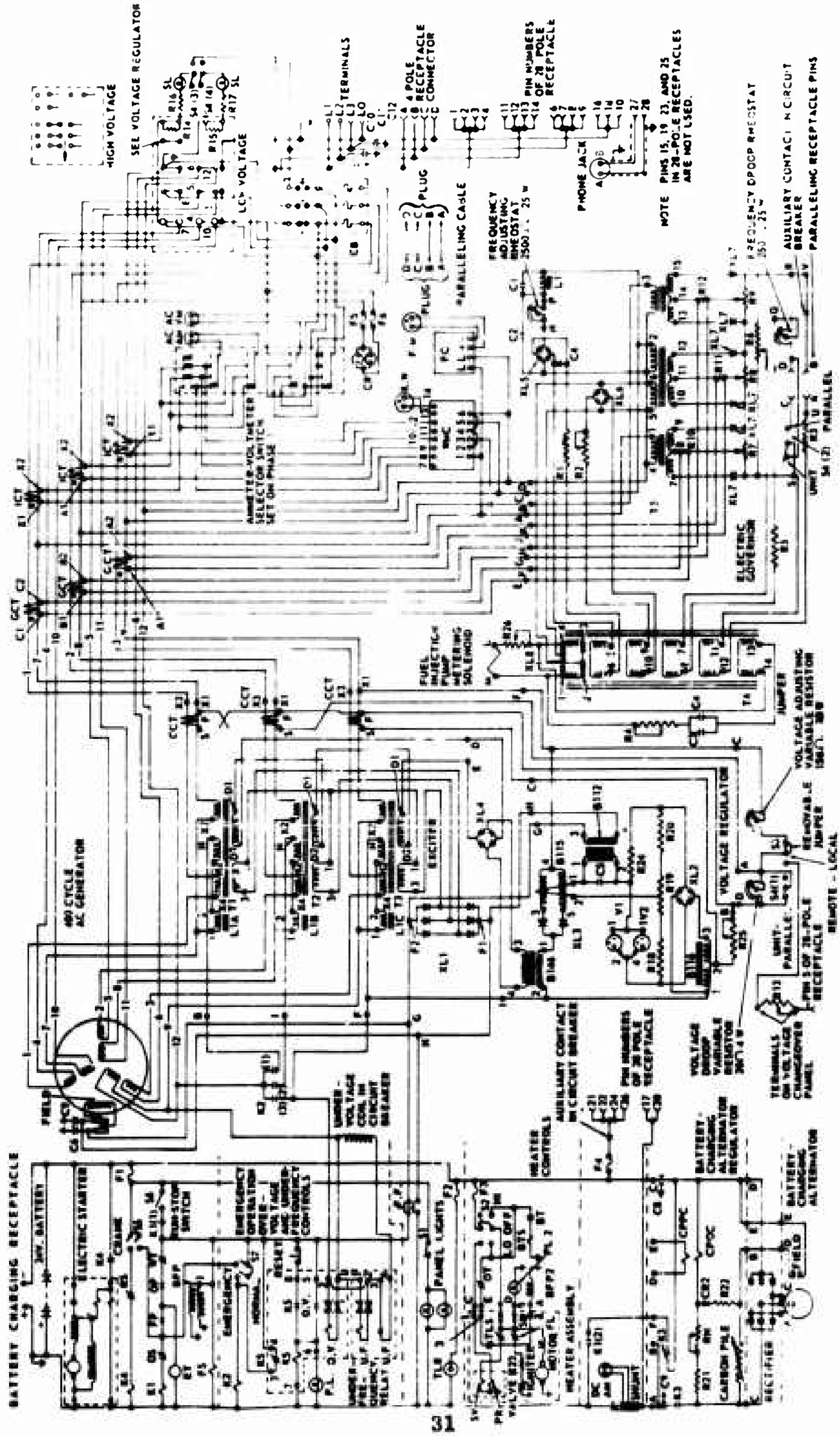

Figure 2.5 Engine-generator-set schematic diagram.

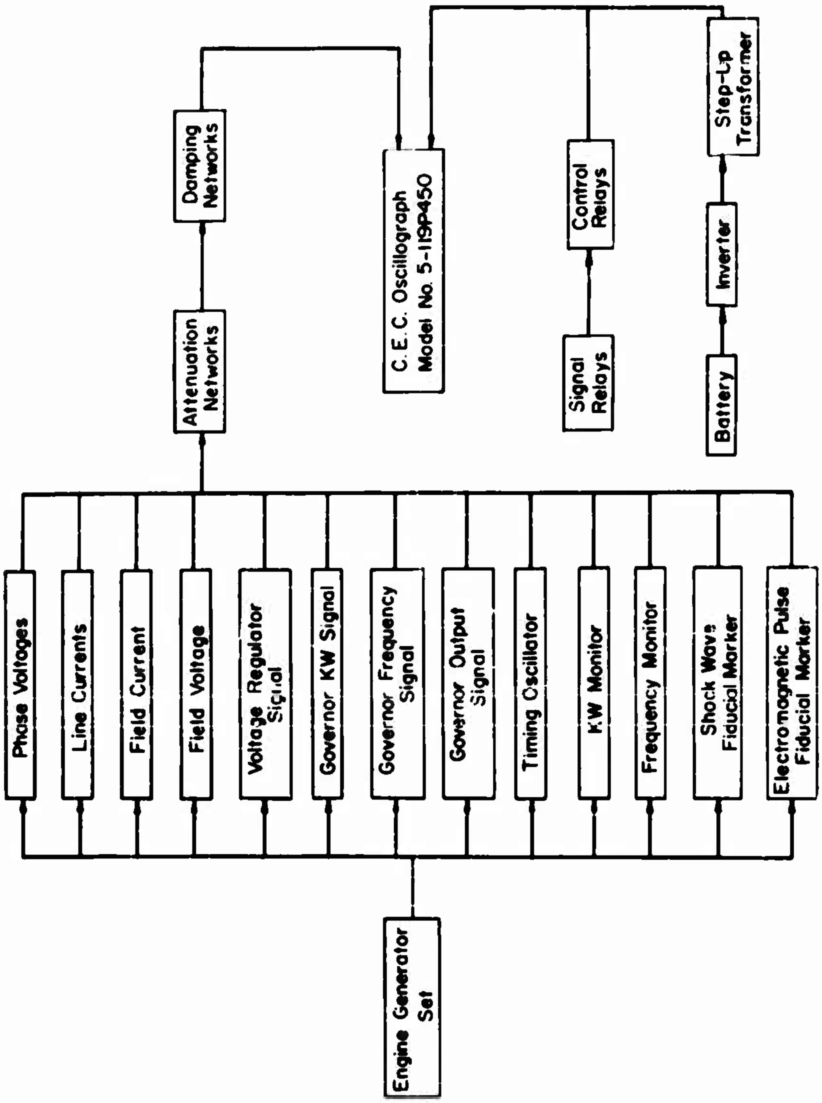

Figure 2.6 Instrumentation system block diagram.

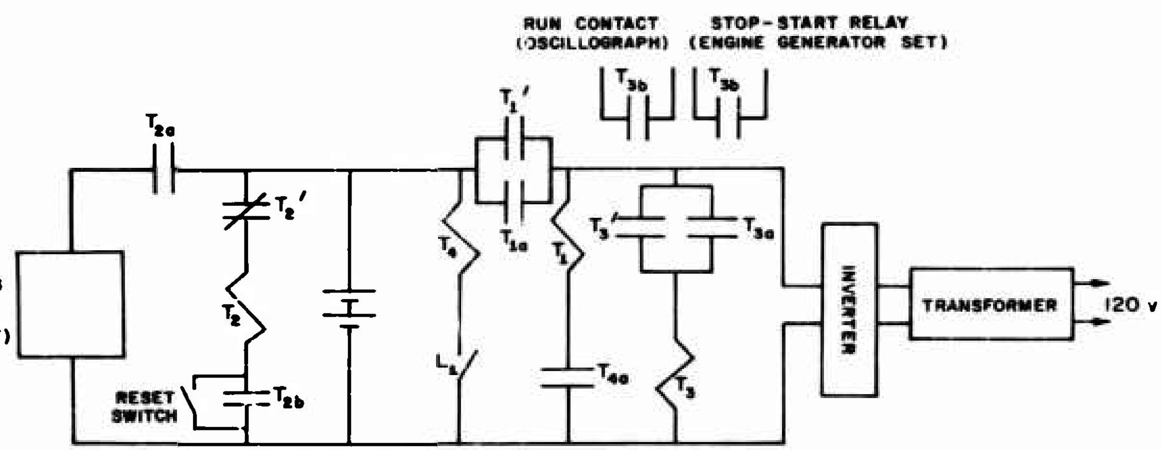

INITIAL RELAY SETTING: Coil T_2 Energized Limit Switch L_1 is closed.

T_1, T_2, T_3, and T_4 Are Instrumentation Relays.

T_1', T_2', T_3', and T_4' Are Timing Signal Relay Contacts.

Figure 2.7 Control relay schematic diagram.

Figure 2.8 Instrumentation package. (USAERDL photo)

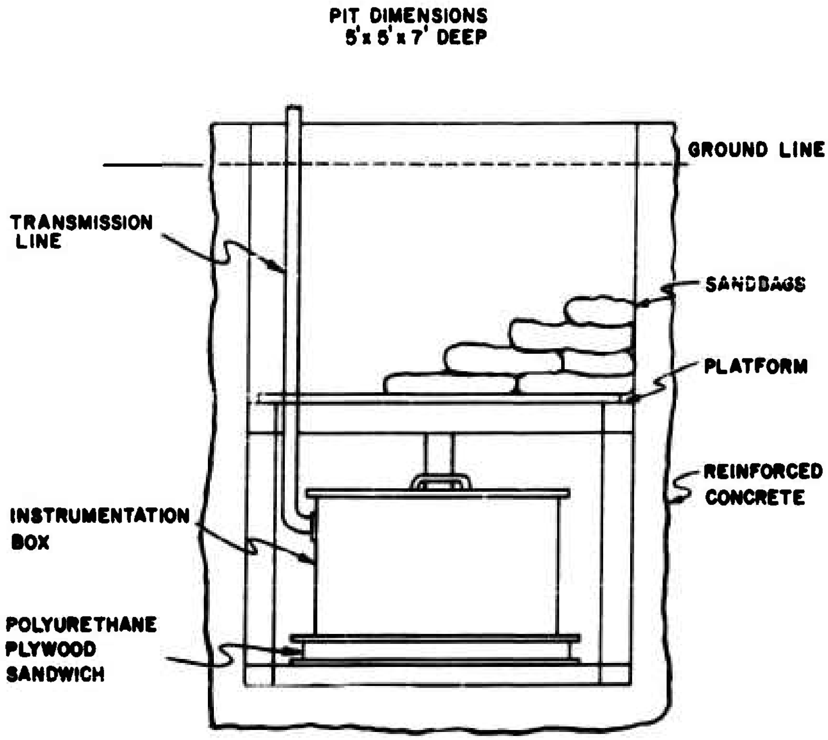

Figure 2.9 Instrumentation station.

CHAPTER 3

RESULTS

3.1 DATA PRESENTATION

Twenty channels of a 50-channel recording oscillograph were used to record the data for this experiment. Two input channels were used to provide zero time reference for the arrival of the electromagnetic pulse and the pressure wave, respectively. One input channel was utilized for the timing oscillator, which provided an accurate timing reference. Seventeen input channels were used to monitor the performance of selected variables. These variables and the recording technique had been chosen to present a complete record of engine-generator set performance during the period from minus 15 seconds to plus 15 seconds and to pinpoint the failure mechanism. The variables can be conveniently grouped into the following categories: output, excitation, and control.

Output variables included line currents as sampled with shunts located directly in the respective lines, line currents as measured with current transformers, phase voltages, power output as determined by computing circuits that provided the input to the kilowatt meter, and frequency as determined by the frequency converter that provided the input to the frequency meter.

Because the generator set under study had a static excitation system in which the excitation was provided by feedback and rectification of a portion of the output signal, excitation performance was represented by studying merely the generator field current and field voltage.

Three important currents within the electric load sensing governor and the current at an informative location in the voltage regulator circuitry comprised the control variables.

The relative position of the oscillogram trace corresponding to each variable was consistent with the above grouping. Table 3.1 contains a summary of the information displayed on each active channel of the oscillograph and the associated calibration data.

3.2 DISCUSSION OF DATA

The data were successfully recovered from the test installation. From preliminary analysis of the data, it has been determined that the instrumentation system functioned properly. The performance of the generator set during the time interval from minus 15 seconds until zero time is demonstrated by the oscillogram shown in Figure 3.1. These data are consistent with other oscillograms recorded under identical conditions of steady-state operation at rated load and power factor. In the time immediately following the arrival of the electromagnetic pulse, the generator set underwent transient behavior and was shut down. Although the data were suitable for analysis, portions of the oscillogram did not result in the quality of data that had been obtained during test runs under similar conditions. It is believed that the lack of quality was caused by subjection of the film to higher temperatures than anticipated during the extensive period when the project was buttoned-up.

Project equipment was returned to USAERDL following decontamination. Laboratory experimentation and data analyses have been conducted to investigate the failure mechanism. In order to prevent having the electrical power system shut down by a relatively minor deviation from normal operating conditions during the period of unattended system operation after evacuation of the area, and in order to obtain maximum information from the experiment, the water temperature, oil pressure, fuel pressure, and overspeed protective devices and the circuit interrupter had been by-passed for the experiment. Consequently, the number of ways in which the electrical power system could have been shut down was very limited.

A detailed physical examination of the generator set revealed that a 30-ampere fuze link was blown. This fuze was located in series with those conductors of the 26-conductor cable which supply direct-current control potential at the load. Further analysis of the oscillogram and the generator set schematic diagram resulted in a postulation for the failure mechanism. The theory postulated was that a current pulse was introduced into the direct-current control circuitry such that control potential to relay KI in Figure 2.5 was modified sufficiently for contacts KI to open. Opening of contacts KI would result in loss of potential to the fuel solenoid (FS), which would result in deactivation of the generator set. In order to investigate the feasibility of this failure mechanism theory, laboratory testing was conducted to determine the circuit interruption time required to result in the opening of contacts K1. The schematic diagram for this investigation is shown in Figure 3.2. The minimum interruption time that would result in the opening of contacts K1 was 1.3 milliseconds.

The next step in the investigation of this failure mechanism theory was to repeat the study of the response of relay K1 to transient control potential interruption under the conditions of power system operation. The findings were identical; the minimum interruption time that resulted in the opening of contacts K1 and the subsequent deactivation of the generator set was found to be 1.3 milliseconds. Furthermore, when the instrumentation system was used to record power-system performance during the control circuit interruption test, the resulting oscillogram was identical to that obtained during the Small Boy experiment. From this result, it was concluded that the basic postulation regarding the failure mechanism was correct.

At this point in the postshot investigations, it had been determined that the failure mechanism was equivalent to the loss of control potential to relay K1 for 1.3 milliseconds. The next step in the investigation was directed toward determination of the characteristics of a current pulse introduced by the cable that would result in the required loss of control potential.

A series of tests on a laboratory scale was devised to further advance the understanding of the postulated shut-down mechanism. The schematic diagram for the laboratory investigation technique is shown in Figure 3.3. A 14μf, 2900-joule, 20-kv capacitor was discharged into the direct-current control circuitry and the transient voltage v(t) was observed on a high-persistence oscilloscope. The series resistor was used to operate on wave shape. Parameters for this investigation were V_o, the initial voltage on the capacitor, and R, the series resistor. Wave shape of the current pulse was largely a function of the energy source parameters because the impedance offered by the lead-acid batteries was much less than the series resistance required for proper wave shaping. Lower voltage discharge measurements were accomplished. It was observed that introduction of the current pulse into the control circuitry resulted in the expected type of transient in voltage v(t). A typical transient waveform for v(t) is shown in Figure 3.4. However, due to the relative magnitude of the control circuitry input impedance and the series resistance required for proper wave-shaping, approximately 80-kv initial voltage would be required for adequate current pulse to lower v(t) sufficiently to investigate the failure mechanism theory. Due to the inconvenience of conducting this experimentation at an 80-kv voltage level, an analog of the sy m was examined.

The equivalent circuit shown in Figure 3.5 was representative of the direct-current control circuitry. R_c and L_c were the coil resistance and coil inductance of relay K1. The other branch was a network representation of the lead acid battery (Reference 4). Other parallel branches were considered negligible. The purpose of this analysis was to determine the $i(t)$ corresponding to the $v(t)$ required to result in the postulated failure mechanism. For the purpose of this analysis, $v(t)$ was assumed to be the first half cycle of a negative sine wave which would decrease the relay potential below the drop-out potential for 1.3 milliseconds. The following equations for the solution of $i(t)$ were formulated by nodal circuit analysis:

$$L_b L_c p^2 i(t) + (R_b L_c + R_c L_b)\, pi(t) + R_b R_c i(t) + (L_c + L_b) pv(t) + (R_b + R_c)\, v(t)$$

$$- L_c\, pv_1(t) - R_c\, v_1(t) = 0$$

$$R_1 C L_b p^2\, v_1(t) + (R_1 C R_b + L_c)\, pv_1(t) + (R_1 + R_b) v_1(t) - R_1\, v(t) = 0$$

where $p = \frac{d}{dt}$ is the Heaviside operator. Development of these equations and the details of the analog program are further explained in the Appendix. The solution for $i(t)$ is shown in Figure 3.6.

An analytical solution for the current pulse required for the postulated failure mechanism was accomplished to verify the analog computer solution. The simplified equivalent circuit used in this analysis is shown in Figure 3.5. As in the analog analysis, $v(t)$ was assumed to be the first half cycle of a negative sine wave which would decrease the relay potential below the drop-out potential for 1.3 milliseconds. The following equation for i(t) was developed by electrical network analysis:

$$i(t)=u(t)\left[58.9\exp(-65t)-739\exp(-7935t)-3625\sin(1610t-10.8^{\circ})\right]$$

$$+u\left(t-\frac{\pi}{1610}\right)\left\{58.9\exp\left[-65\left(t-\frac{\pi}{1610}\right)\right]-739\exp\left[-7935\left(t-\frac{\pi}{1610}\right)\right]\right.$$

$$\left.-3625\sin\left[1610\left(t-\frac{\pi}{1610}\right)-10.8^{\circ}\right]\right\}$$

Details of the analytical solution are shown in the Appendix.

The solution for i(t) was identical to that obtained from the analog computer analysis and is shown in Figure 3.6. The peak value of i(t) as determined from the digital computer readout was 3570 amperes.

TABLE 3.1 SUMMARY OF OSCILLOGRAM VARIABLES AND CALIBRATION DATA

Oscillogram Trace	Variable	Variable Group	Direct Current Deflection Level (inches)	Calibration Factor
1,2,3	Line Currents (Shunt Measurements)	Output	0	256 amp/in
4,5,6	Phase Voltages	Output	0	167 v/in
7,8,9	Line Currents (Current Transformer Measurement)	Output	0	183 amp/in
10	Kilowatt Monitor	Output	0	2.0 ma/in
11	Frequency Current	Output	2.60	38.5 μa/in (dc)
12	Field Current	Excitation	1.12	23.2 amp/in (dc)
13	Field Voltage	Excitation	2.34	22.2 v/in (dc)
14	Voltage Regulator	Control	1.46	0.686 amp/in (dc)
15	Governor	Control	0.07	62.3 ma/in (dc)
16	Governor Frequency	Control	0.40	15.48 ma/in (dc)
17	Governor Solenoid	Control	2.32	215.5 ma/in (dc)
18	Electromagnetic Pulse Arrival	Fiducial Marker	0	N/A
19	Pressure Wave Arrival	Fiducial Marker	0	N/A
20	Timing Reference	Fiducial Marker	0	N/A

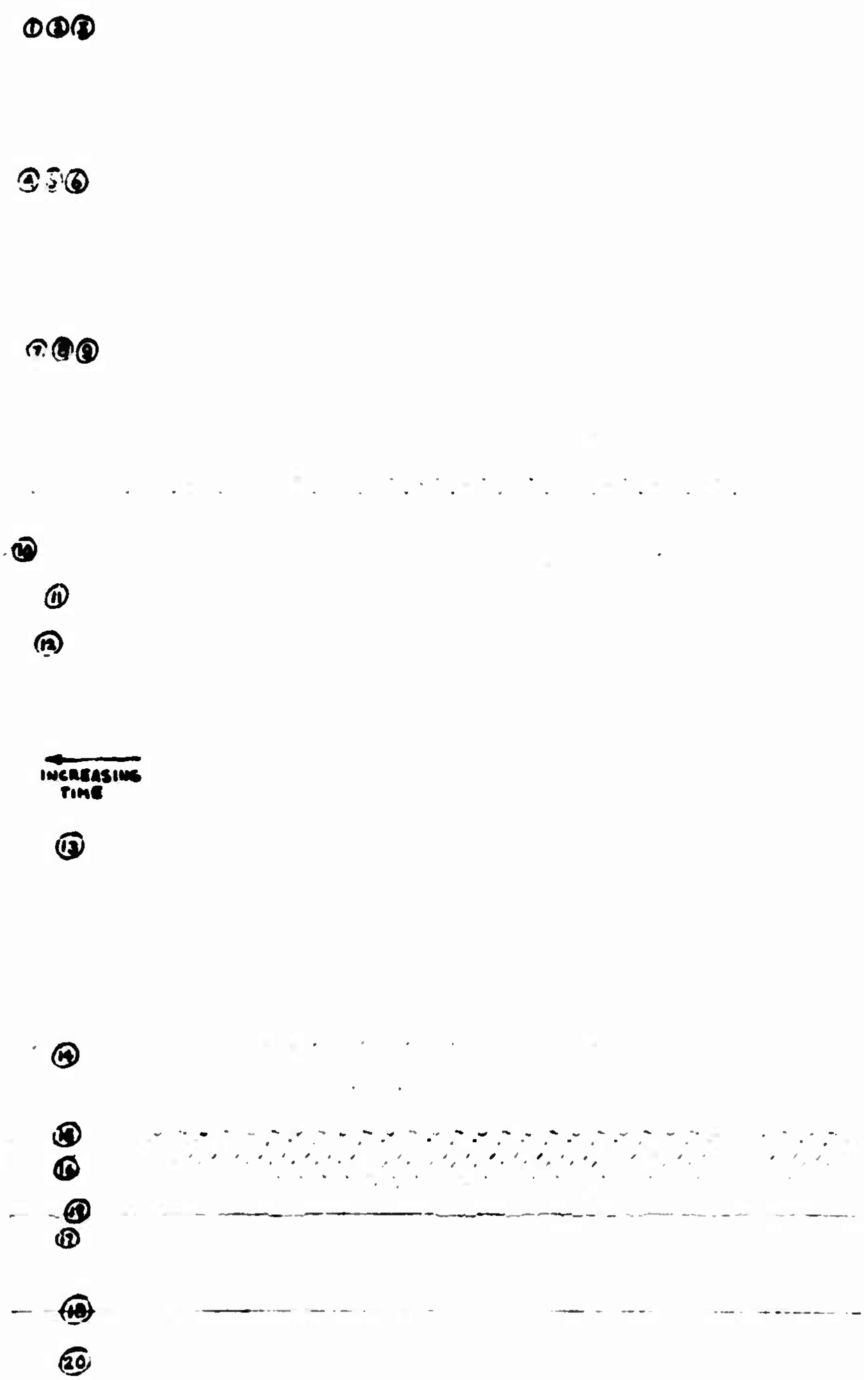

Figure 3.1 Oscillogram of predetonation steady-state performance.

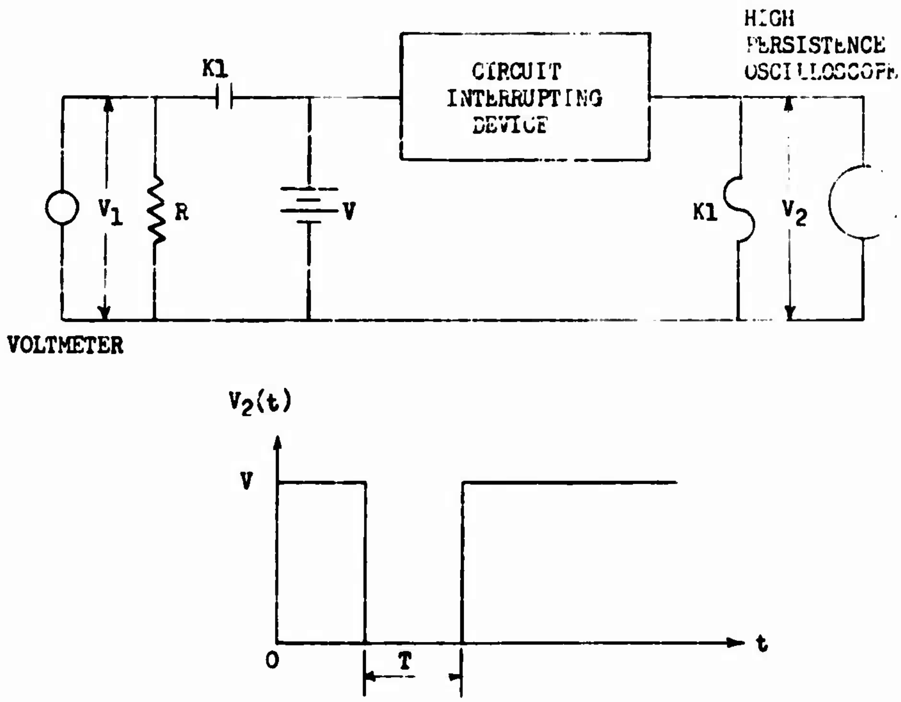

Figure 3.2 Schematic diagram for laboratory investigation of relay response to circuit interruption.

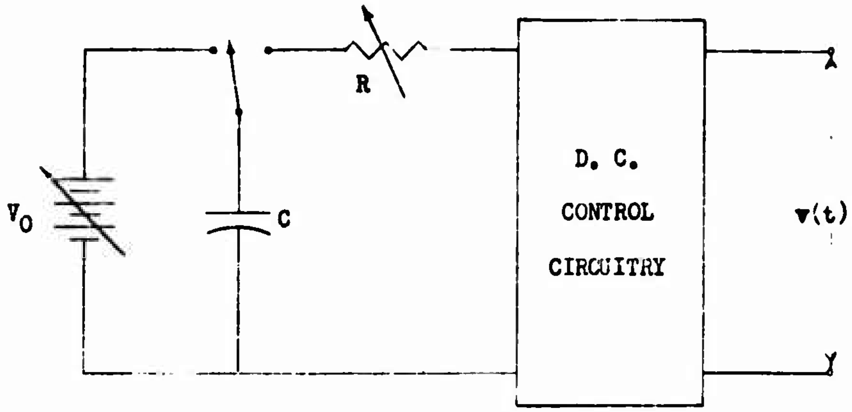

Figure 3.3 Schematic diagram for pulse testing of control circuitry.

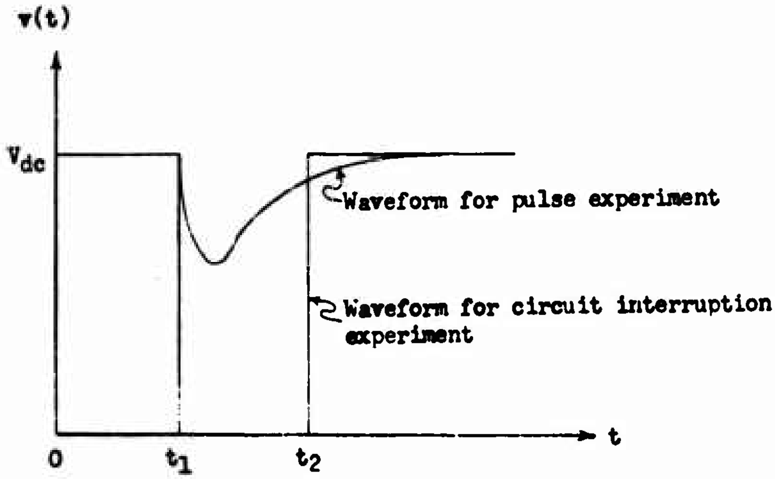

Figure 3.4 Typical waveforms for v(t) obtained during laboratory tests.

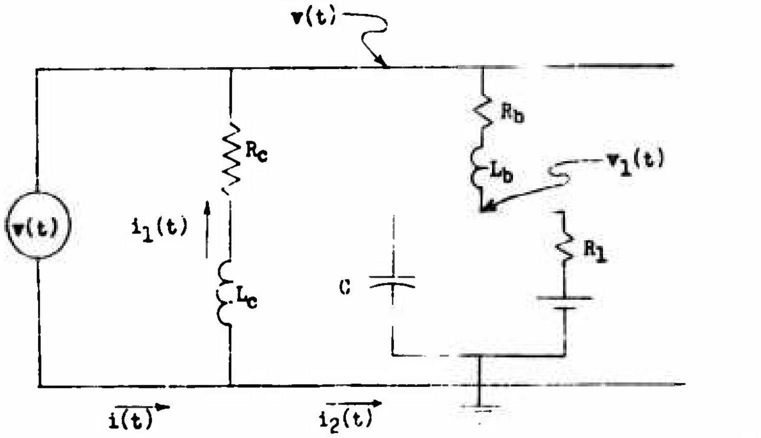

$v(t) = 0, \qquad t < 0,\ t > \pi/1.61\times10^3$

$v(t) = 30 \sin(1.61 \times 10^3)t \qquad 0 \leq t \leq \pi/1.61\times10^3$

$L_b = 10^{-6}$ henry $\qquad R_b = 8\ (10)^{-3}$ ohm

$L_c = 0.52$ henry $\qquad R_1 = 5\ (10)^{-3}$ ohm

$R_c = 225$ ohms $\qquad C = 5$ farads

Figure 3.5 Equivalent circuit for analog computer analysis and transient circuit analyses.

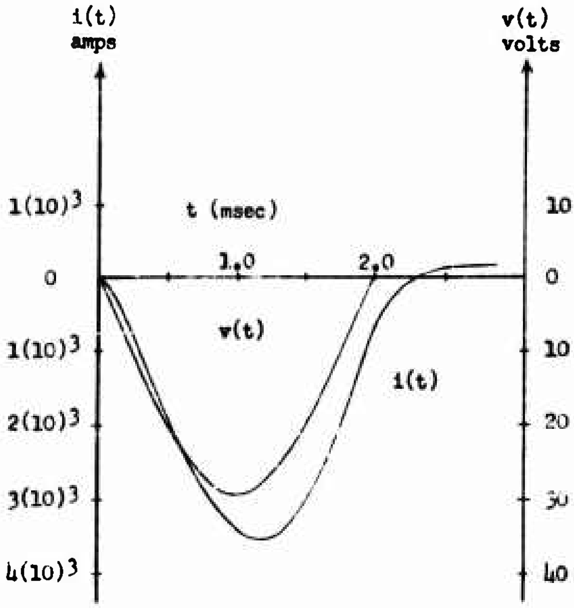

Figure 3.6 Solution for i(t) as determined by analog computer and transient analyses.

CHAPTER 4

CONCLUSIONS

The transient environment to which the electrical power system was subjected as a result of the nuclear detonation was very complicated, and a quantitative analysis of the response of the system to this transient environment was not a straightforward process. From the test results and the postshot laboratory experimentation and analyses, it was concluded that shut down of the electrical power system was caused by the opening of relay contacts K1 by a combination of effects such as prompt radiation, interaction of the transient magnetic field with the magnetic field of the relay, and currents induced in the distribution cables by the electromagnetic environment of which the latter was concluded to be the major contributing factor. From the laboratory experimentation and analyses conducted in conjunction with this report, it was concluded that if induced currents in the distribution cables were the only cause of power system shut down, a current pulse of approximately 3,570 amperes maximum would be required. This experiment has demonstrated that field army electrical power systems are vulnerable to electromagnetic effects of nuclear detonations. Results of this experiment will be applied to a related Nuclear Weapons Effects Research program at USAERDL.

ANALYTICAL AND ANALOG COMPUTER DEVELOPMENTS FOR CURRENT PULSE CHARACTERISTICS

Refer to Figure 3.5 for notation.

$$i(t) = i_1(t) + i_2(t) \qquad 1.00$$

Taking the Laplace transform of eq. 1.00

$$\mathcal{L}\{f(t)\} = \int_0^\infty f(t)\, e^{-s\tau}\, d\tau = F(s)$$

$$I(s) = I_1(s) + I_2(s) = V(s)\left[\frac{1}{Z_1(s)} + \frac{1}{Z_2(s)}\right] \qquad 1.01$$

$$Z_1(s) = R_c + sL_c \qquad 1.02a$$

$$Z_2(s) = R_b + sL_b + \frac{R_1/sC}{R_1 + 1/sC} = \frac{(sL_b + R_b)(sCR_1 + 1) + R_1}{sCR_1 + 1} \qquad 1.02b$$

$$v(t) = -A \sin\omega t\, u(t) - A \sin\omega t\, u(t-\tau) \qquad \tau = \pi/\omega \qquad 1.02c$$

$$V(s) = \frac{-A\omega}{s^2+\omega^2} - \frac{A\omega e^{-s\tau}}{s^2+\omega^2} = \frac{-A\omega}{s^2+\omega^2}\left(1 + e^{-s\tau}\right) \qquad 1.02d$$

Inserting eqs. 1.02 into eq. 1.01

$$I(s) = \frac{-A\omega}{s^2+\omega^2}\left(1 + e^{-s\tau}\right)\left[\frac{1}{sL_c + R_c} + \frac{sCR_1 + 1}{(sL_b + R_b)(sCR_1 + 1) + R_1}\right]$$

$$I(s) = \frac{-A\omega}{s^2+\omega^2}\left(1 + e^{-s\tau}\right)\left[\frac{s^2(L_bCR_1 + L_cCR_1) + s(CR_1R_b + L_b + CR_1R_c + L_c) + R_b + R_1 + R_c}{(sL_c + R_c)\left[(sL_b + R_b)(sCR_1 + 1) + R_1\right]}\right] \qquad 1.03$$

$$L_cCR_1 \gg L_bCR_1 \qquad 1.04a$$

$$L_c \gg L_b \qquad 1.04b$$

$$R_1R_cC \gg R_1R_bC \qquad 1.04c$$

$$R_c \gg R_b + R_1 \qquad 1.04d$$

$$R_1R_cC \gg L_b \qquad 1.04e$$

Inserting inequalities 1.04 into eq. 1.03

$$I(s) = \frac{-A\omega}{s^2+\omega^2}\left(1+e^{-s\tau}\right)\frac{(sCR_1+1)(sL_c+R_c)}{(sL_c+R_c)\left[(sL_b+R_b)(sCR_1+1)+R_1\right]}$$

$$= \frac{-A\omega}{s^2+\omega^2}\left(1+e^{-s\tau}\right)\frac{sCR_1+1}{s^2L_bCR_1+s(CR_bR_1+L_b)+R_b+R_1}$$

$$I(s) = F(s) + F(s)\,e^{-s\tau} \qquad 1.05$$

$$F(s) = -\frac{A\omega}{L_b}\frac{\left(s+\frac{1}{R_1C}\right)}{(s^2+\omega^2)\left[s^2+s\,\frac{CR_bR_1+L_b}{L_bCR_1}+\frac{R_b+R_1}{L_bCR_1}\right]}$$

$$F(s) = \frac{-\delta(s+\nu)}{(s^2+\omega^2)\left[s^2+\xi s+\eta\right]} = \frac{-\delta(s+\nu)}{(s^2+\omega^2)(s+\alpha)(s+\beta)} \qquad 1.06$$

Where

$$\delta = \frac{A\omega}{L_b} = \frac{(30)(1.61)(10)^3}{10^{-6}} = 4.83(10)^{10} \qquad 1.07a$$

$$\nu = \frac{1}{R_1C} = \frac{1}{(5)(10)^{-3}(5)} = 40 \qquad 1.07b$$

$$\omega = 1.61(10)^3 \qquad 1.07c$$

$$\xi = \frac{CR_bR_1+L_b}{L_bCR_1} = \frac{(5)(8)(10)^{-3}(5)(10)^{-3}+10^{-6}}{(10)^{-6}(5)(5)(10)^{-3}} \doteq 8(10)^3 \qquad 1.07d$$

$$\eta = \frac{R_b+R_1}{L_bCR_1} = \frac{8(10)^{-3}+5(10)^{-3}}{(10)^{-6}(5)(5)(10)^{-3}} = 5.2(10)^5 \qquad 1.07e$$

$$s^2+\xi s+\eta = s^2+8(10)^3+5.2(10)^5 = (s+\alpha)(s+\beta)$$

$$-\alpha,-\beta = \frac{-8(10)^3 \pm \sqrt{64(10)^6-(4)(1)(5.2)(10)^5}}{2(1)} = -65,\ -7.935(10)^3$$

$$\alpha = 65 \qquad \beta = 7.935(10)^3 \qquad 1.07f$$

Inserting eqs. 1.07 into eq. 1.06

$$F(s) = \frac{-4.83\,(10)^{10}\,(s+40)}{\left\{s^2+\left[1.61\,(10)^3\right]^2\right\}\left[s+65\right]\left[s+7.935\,(10)^3\right]} \qquad 1.08$$

Taking the inverse Laplace Transform of eq. 1.08

$$\mathcal{L}^{-1}\left\{F(s)\right\} = f(t) = \left[A e^{-\alpha t} + B e^{-\beta t} + C \sin(\omega t+\phi)\right](-\delta)\, u(t) \qquad 1.08a$$

Where

$$A = \frac{\nu-\alpha}{(\beta-\alpha)(\alpha^2+\omega^2)} = -1.22\,(10)^{-9} \qquad 1.09a$$

$$B = \frac{\nu-\beta}{(\alpha-\beta)(\beta^2+\omega^2)} = 1.529\,(10)^{-8} \qquad 1.09b$$

$$C = \frac{1}{\omega}\left[\frac{\nu^2+\omega^2}{(\alpha^2+\omega^2)(\beta^2+\omega^2)}\right]^{1/2} = 7.51\,(10)^{-8} \qquad 1.09c$$

$$\phi = \tan^{-1}\left(\frac{\beta}{\omega}\right) - \tan^{-1}\left(\frac{\omega}{\alpha}\right) - \tan^{-1}\left(\frac{\nu}{\omega}\right) = -10.8^\circ \qquad 1.09d$$

Inserting eqs. 1.09 into eq. 1.08a

$$f(t) = \left\{58.9\, e^{-65t} - 739\, e^{-7935t} - 3625 \sin\left[(1.61)(10)^3 t - 10.8^\circ\right]\right\} u(t) \qquad 1.10$$

Taking the inverse Laplace transform of eq. 1.05

$$i(t) = f(t) + f(t-\tau) \qquad 1.11$$

Inserting eq. 1.10 into eq. 1.11 results in the following solution for $i(t)$

$$i(t) = \left[58.9\, e^{-65t} - 739\, e^{-7935t} - 3625 \sin(1610t - 10.8^\circ)\right] u(t)$$
$$+\left\{58.9\, e^{-65(t-\pi/1610)} - 739\, e^{-7935(t-\pi/1610)} - 3625 \sin\left[1610(t-\pi/1610) - 10.8^\circ\right]\right\} u(t-\pi/1610)$$

ANALOG COMPUTER DEVELOPMENT FOR CURRENT PULSE CHARACTERISTICS

Refer to Figure 3.5 for notation

Writing nodal equations with $p = \frac{d}{dt}$

$$i(t) + \frac{v(t) - 0}{pL_c + R_c} + \frac{v(t) - v_1(t)}{pL_b + R_b} = 0 \qquad 1.1a$$

$$\frac{v_1(t) - v(t)}{pL_b + R_b} + pC\,(v_1(t) - 0) + \frac{v_1(t) - 0}{R_1} = 0 \qquad 1.2a$$

Rearranging eqs. 1.1a and 1.2a

$$p^2 L_b L_c\, i(t) + p\,(R_b L_c + R_c L_b)\, i(t) + R_b R_c\, i(t) + (L_c + L_b)\, p\, v(t)$$
$$+ (R_b + R_c)\, v(t) - p L_c\, v_1(t) - R_c\, v_1(t) = 0 \qquad 1.1b$$

$$p^2 R_1 C L_b\, v_1(t) + p\,(R_1 C R_b + L_c)\, v_1(t) + (R_1 + R_b)\, v_1(t) - R_1\, v(t) = 0 \qquad 1.2b$$

Solving eqs. 1.1b and 1.2b for the highest order derivatives:

$$p^2 i(t) = -\frac{(R_b L_c + R_c L_b)}{L_b L_c}\, p\, i(t) - \frac{R_b R_c}{L_b L_c}\, i(t) - \frac{(L_c + L_b)}{L_b L_c}\, p\, v(t)$$
$$- \frac{(R_b + R_c)}{L_b L_c}\, v(t) + \frac{L_c}{L_b L_c}\, p\, v_1(t) + \frac{R_c}{L_b L_c}\, v_1(t) \qquad 1.1c$$

$$p^2 v_1(t) = \frac{-(R_1 C R_b + L_c)}{R_1 C L_b}\, p\, v_1(t) - \frac{(R_1 + R_b)}{R_1 C L_b}\, v_1(t) + \frac{R_1}{R_1 C L_b}\, v(t) \qquad 1.2$$

Inserting the parameter values into eqs. 1.1c and 1.2c:

$$p^2 i(t) = -0.8433\, p\, i(t) - 0.0346\, i(t) - 100\, p\, v(t) - 4.33\, v(t)$$

$$+ 100\, p\, v_1(t) + .33\, v_1(t) \qquad 1.1\,d$$

$$p^2 v_1(t) = -2.08(10)^7\, p\, v_1(t) - 5.2(10)^5\, v_1(t) + (10)^5\, v(t) \qquad 1.2\,d$$

The signal flow chart used for the analog computer solution of eqs 1.1d and 1.2d is shown in Figure A.1

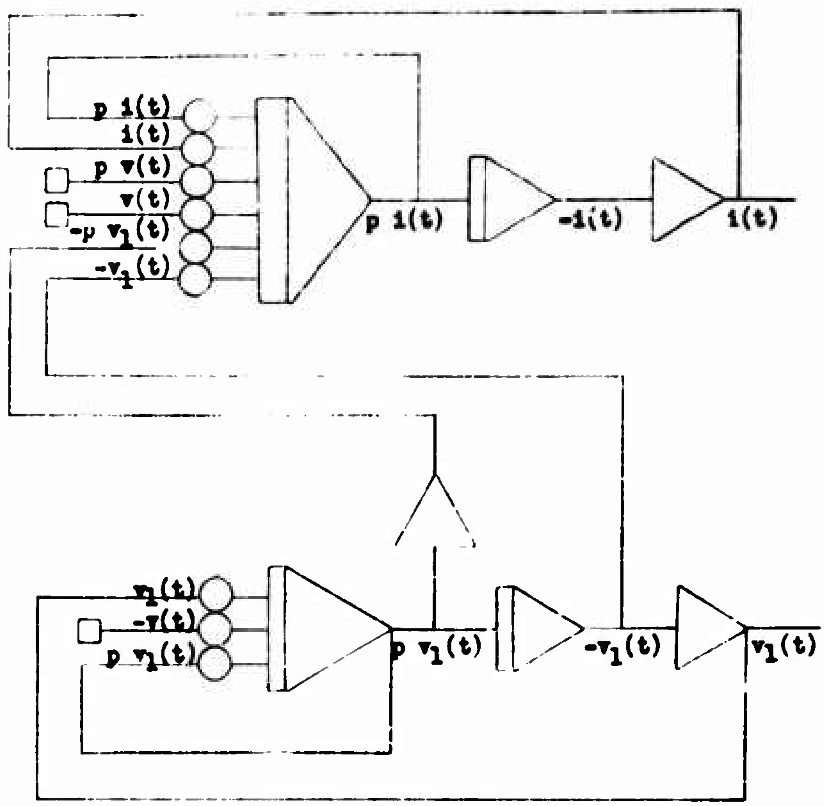

Figure A.1 Flow chart for analog computer solution for i(t).

REFERENCES

1. P. H. Haas and F. N. Wimenitz; "Measurement of the Magnetic Component of the Electromagnetic Field Near a Nuclear Detonation', Project 6.2, Operation Plumbbob, WT -1436, May 1962; Diamond Ordnance Fuze Laboratories, Washington, D. C.; Secret.
2. Research Directorate, AFSWC; "Small Boy Pretest Analysis"; Planning Report No. 1; 6 April 1962; Weapons Effects and Tests Group, Headquarters, Field Command, DADA, Sandia Base, New Mexico; Secret, Restricted Data
3. J. A. Stratton; "Electromagnetic Theory"; McGraw Hill Book Company; 1941
4. W. H. Cox, H. E. Fletcher, and J. E. Partch; Bridge Measurements of Impedance and Determination of Equivalent Circuit of a Primary Silver-Zinc Battery": AIEE Conference Paper No. CP 62-1152; May 1962

DISTRIBUTION

Military Distribution Category [illegible]

ARMY ACTIVITIES

1 CHIEF OF R & D DA
2 DC OF S FOR MIL OPS DA ATTN DIR OF CRR
3 CHIEF OF ENGINEERS DA
4- 5 ARMY MATERIEL COMMAND
6 CHIEF SIGNAL OFFICER DA
7 CHIEF OF TRANSPORTATION DA
8 THE SURGEON GENERAL DA
9- 10 U S ARMY COMBAT DEVELOPMENTS COMMAND
11 DIRECTOR OF SPECIAL WEAPONS DEVELOPMENT OFFICE
12 U S ARMY ARTILLERY BOARD
13 U S ARMY INFANTRY BOARD
14 U S ARMY AIR DEFENSE BOARD
15 U S ARMY COMMAND AND GENERAL STAFF COLLEGE
16 U S ARMY AIR DEFENSE SCHOOL
17 U S ARMY ARMORED SCHOOL
18 U S ARMY ARTILLERY & MISSILE SCHOOL
19 U S ARMY AVIATION SCHOOL
20 U S ARMY INFANTRY SCHOOL
21 U S MILITARY ACADEMY
22 QUARTERMASTER SCHOOL U S ARMY
23 U S ARMY ORDNANCE & GUIDED MISSILE SCHOOL
24 CHEMICAL CORPS TRAINING CMD
25 U S ARMY SIGNAL SCHOOL
26 U S ARMY TRANSPORTATION SCHOOL
27 ENGINEER SCHOOL
28 MEDICAL FIELD SERVICE SCHOOL
29 U S ARMY NUCLEAR MEDICINE RESEARCH DET EUROPE
30 ARMED FORCES INSTITUTE OF PATH
31 ARMY MEDICAL RESEARCH LAB
32 WALTER REED ARMY INST OF RES
33 GENERAL SUPPLIES RESEARCH & ENGINEERING LAB
34 ENGINEER RESEARCH & DEV LAB
35 WATERWAYS EXPERIMENT STATION
36 PICATINNY ARSENAL
37 DIAMOND ORDNANCE FUZE LABORATORY
38- 39 BALLISTIC RESEARCH LABORATORY
40 FRANKFORD ARSENAL
41 WATERVLIET ARSENAL
42- 44 U S ARMY MISSILE COMMAND
45 U S ARMY MOBILITY COMMAND
46 ORDNANCE AMMUNITION COMMAND
47 U S ARMY WEAPONS COMMAND
48 U S ARMY MUNITIONS COMMAND
49 COMMUNICATIONS & ELECTRONICS COMMAND
50 U S ARMY ELECTRONIC PROVING GROUND
51 U S ARMY SIGNAL R&D LABORATORY
52 U S ARMY TRANSPORTATION RESEARCH COMMAND
53 U S ARMY TRANSPORTATION COM [illegible] DEVELOPMENT GROUP
54 THE RESEARCH & ANALYSIS CORP
55 WHITE SANDS SIGNAL SUPPORT AGENCY
56 NUCLEAR DEFENSE LABORATORY
57 U S ARMY AIR DEFENSE COMBAT DEV AGENCY

NAVY ACTIVITIES

58- 59 CHIEF OF NAVAL OPERATIONS OP03EG
60 CHIEF OF NAVAL OPERATIONS OP-31
61 CHIEF OF NAVAL OPERATIONS OP-75
62 CHIEF OF NAVAL OPERATIONS OP-91
63 CHIEF OF NAVAL OPERATIONS OP-922G1
64- 65 CHIEF OF NAVAL RESEARCH
66- 68 BUREAU OF NAVAL WEAPONS DLI-3
69 BUREAU OF MEDICINE & SURGERY
70 BUREAU OF SHIPS CODE 423
71 BUREAU OF YARDS & DOCKS
72 U S NAVAL RESEARCH LABORATORY
73- 74 U S NAVAL ORDNANCE LABORATORY
75 NAVY ELECTRONICS LABORATORY
76 U S NAVAL MINE DEFENSE LAB
77- 78 U S NAVAL RADIOLOGICAL DEFENSE LAB
79 U S NAVAL CIVIL ENGINEERING LAB
80 U S NAVAL SCHOOLS COMMAND TREASURE ISLAND
81 U S NAVAL POSTGRADUATE SCHOOL
82 NUCLEAR WEAPONS TRAINING CENTER ATLANTIC
83 NUCLEAR WEAPONS TRAINING CENTER PACIFIC
84 U S NAVAL DAMAGE CONTROL TNG CENTER
85 NAVAL AIR MATERIAL CENTER
86 U S NAVAL AIR DEVELOPMENT CENTER
87 U S NAVAL AIR SP WPNS FACILITY
88 U S NAVAL MEDICAL RESEARCH INSTITUTE
89 DAVID W TAYLOR MODEL BASIN
90 U S NAVAL SUPPLY R&D FACILITY
91- 94 U S MARINE CORPS CODE A03H

AIR FORCE ACTIVITIES

95 HQ USAF AFRDC-AE
96 HQ USAF AFRDR-NU
97 HQ USAF OPERATIONS ANALYSIS OFFICE
98-102 HQ USAF AFCIN-3D1
103 AC OF S INTELLIGENCE
104 DC OF S RESEARCH & TECHNOLOGY
105 THE SURGEON GENERAL
106 TACTICAL AIR COMMAND
107 AIR DEFENSE COMMAND
108 AIR FORCE SYSTEMS COMMAND
109 AIR FORCE BALLISTIC SYSTEMS DIVISION
110 RADC-RAALD,GRIFFISS AFB
111 PACIFIC AIR FORCES
112-113 AF CAMBRIDGE RESEARCH CENTER
114-118 AFSWC KIRTLAND AFB WREX
119-120 AIR UNIVERSITY LIBRARY
121 LOWRY AFB
122 SCHOOL OF AVIATION MEDICINE
123-125 AERONAUTICAL SYSTEMS DIVISION
126-127 USAF PROJECT RAND
128 AIR TECHNICAL INTELLIGENCE CENTER
129 OFFICE OF AEROSPACE RESEARCH

OTHER DEPARTMENT OF DEFENSE ACTIVITIES

130 DIRECTOR OF DEFENSE RESEARCH AND ENGINEERING
131 ASST TO THE SECRETARY OF DEFENSE ATOMIC ENERGY
132 ADVANCE RESEARCH PROJECT AGENCY
133 WEAPONS SYSTEM EVALUATION GROUP
134-137 DEFENSE ATOMIC SUPPORT AGENCY
138 FIELD COMMAND DASA
139 FIELD COMMAND DASA FCTG
140-141 FIELD COMMAND DASA FCWT
142-143 DEFENSE INTELLIGENCE AGENCY
144 ARMED SERVICES EXPLOSIVES SAFETY BOARD
145 JOINT TASK FORCE-8
146 COMMANDER-IN-CHIEF EUCOM
147 COMMANDER-IN-CHIEF PACIFIC
148 COMMANDER-IN-CHIEF ATLANTIC FLEET
149 STRATEGIC AIR COMMAND
150 CINCONAD
151-153 ASST SECRETARY OF DEFENSE CIVIL DEFENSE

ATOMIC ENERGY COMMISSION ACTIVITIES

154-156 AEC WASHINGTON TECH LIBRARY
157-158 LOS ALAMOS SCIENTIFIC LAR

159-163 SANDIA CORPORATION
164-175 LAWRENCE RADIATION LAB LIVERMORE
176-177 NEVADA OPERATIONS OFFICE,LAS VEGAS

FOR CIVILIAN DISTR CAT. B 2

178 FORD MOTOR CO NEWPORT BEACH CALIF ATTN ROHLIG
179 SPACE GEN CORP ELMONTE CALIF ATTN BROWN
180 GEC TECH MIL PL OP SANTA BRABARA CALIF HEDGES
181 GEC TECH MIL PL OP SANTA BRABARA CALIF CHAN
182 GEC TECH MIL PL OP SANTA BRABARA CALIF FISCHER
183 GEC TECH MIL PL OP SANTA BRABARA CALIF HART
184 BENDIX SYSTEMS DIV ANN ARBOR MICH ATTN COLVIN
185 RADIATION EFFECTS OPERATION GEC SYRACUSE ATTN BUIE
186 KAMAN NUCLEAR COL.SPRINGS COL. ATTN BITTNER
187 KAMAN NUCLEAR COL.SPRINGS COL. ATTN MOORHEAD
188 RAND CORP SANTA MONICA ATTN TAMARKIN
189 HQ/FAA ATTN LT COL OGLE WASHINGTON
190-191 BELL TELEPHONE LAB MURRY HILL N J ATTN SCHWARTZ,INS
192-193 UNIV OF CALIF LRL LIVERMORE ATTN WATSON,WOUTENS
194-196 LASL LOS ALAMOS ATTN SUYDAM,MALIK,LONGMIRE
197 DIR NATIONAL SECURITY AGENCY FT GEO MEADE ATTN SLOA
198-199 HUGHES AIRCRAFT CO FULLERTON CALIF ATTN LOWRY,HANSC
200 THE MITRE CO BEDFORD MASS ATTN GRANT
201 SPACE TECH LAB REDONDO BEACH CALIF ATTN MATHEWS
202 SPACE TECH LAB REDONDO BEACH CALIF ATTN PUGSLEY
203 SPACE TECH LAB REDONDO BEACH CALIF ATTN NORTON
204 BELL TELEPHONE LAB INC WHIPPANY N J ATTN MIDDAUGH
205 DENVER RESEARCH INSTITUTE UNIV DENV.ATTN FOWLES
206 NORTHROP VENTURA VAN NUYS CALIF ATTN BROWN
207 SPACE GUIDANCE CENTER IBM OWEGO N Y ATTN KLUEPPER
208 BOEING COMPANY SEATTLE WASH ATTN BRYSON
209 BOEING COMPANY SEATTLE WASH ATTN KEISTER
210 BOEING COMPANY SEATTLE WASH ATTN REED
211 HUGHES AIRCRAFT CO FULLERTON CALIF ATTN HOFFMAN
212 NSA WASHINGTON ATTN COL EDWARDS
213 PRES.SANDIA CORP ALBUQUERQUE ATTN FLANAGAN
214 PRES.SANDIA CORP ALBUQUERQUE ATTN KAMBOURELIS
215 PRES.SANDIA CORP ALBUQUERQUE ATTN EASLEY
216 PRES.SANDIA CORP ALBUQUERQUE ATTN COOK
217 STANFORD RES INST MENLO PARK CALIF ATTN DOC CUST PO
218 CALIF INST OF TECH PASADENA ATTN CHRISTY
219 US GEO SURVEY DENVER ATTN BLACK
220 CHIEF DASA WASHINGTON FOR AWRE ENG
221 CHIEF DASA WASHINGTON FOR MIN OF AVIATION ENG
222 SPACE TECH LAB WASHINGTON ATTN SUSSHOLZ
223 NORTHROP CORP CORP WASHINGTON ATTN O DELL
224 AIR TECH CORP CAMBRIDGE MASS ATTN CLAPP
225 DTIE OAK RIDGE,MASTER
226-295 DTIE OAK RIDGE SURPLUS

CONFIDENTIAL